JPP Journal of Pharmacy and Pharmacology

JPP 2004, 56: 351–358

Received July 24, 2003
Accepted December 03, 003
DOI 10.1211/0022357022908

Systemic and ocular pharmacokinetics of *N*-4-benzoylaminophenylsulfonylglycine (BAPSG), a novel aldose reductase inhibitor

Gangadhar Sunkara, Surya P. Ayalasomayajula, Cheruku S. Rao, Jonathan L. Vennerstrom, Jack DeRuiter and Uday B. Kompella

Abstract

To better develop *N*-[4-(benzoylamino)phenylsulfonyl]glycine (BAPSG), a potent and selective aldose reductase inhibitor capable of delaying the progression of ocular diabetic complications, the objective of this study was to assess its pharmacokinetics. The plasma pharmacokinetics of BASPG was assessed in male Sprague-Dawley rats following intravenous, intraperitoneal and oral routes of administration and its distribution to various tissues including those of the eye was studied following intraperitoneal administration. In addition, rat plasma protein binding of BAPSG was studied using ultracentrifugation method and its ocular tissue disposition was assessed following topical administration in rabbits. Plasma and tissue levels of BAPSG were analysed using an HPLC assay. BAPSG exhibited dose-proportionate $AUC_{0-\infty}$ (area under the plasma concentration–time curve) following both intravenous and intraperitoneal administration over the dose range (5–50 mg kg^{-1}) studied and an erratic oral absorption profile with low oral bioavailability. The fraction bioavailability following oral and intraperitoneal administration was 0.06 and 0.7–1, respectively. BAPSG exhibited short plasma elimination half-lives in the range 0.5–1.5 h. BAPSG was bound to rat plasma proteins and the percent protein binding ranged from 83 to 99.8%. BAPSG was better distributed to cornea, lens and retina than to brain, following intraperitoneal administration in rats. However, the distribution was lower compared with kidney and liver. Following topical administration in rabbits, BAPSG delivery to the surface ocular tissues, cornea and conjunctiva was higher compared with intraocular tissues, aqueous humour, iris-ciliary body and lens. Thus, BAPSG was distributed to ocular tissues following systemic and topical modes of administration.

Department of Pharmaceutical Sciences, University of Nebraska Medical Center, Omaha, NE 68198-6025, USA

Gangadhar Sunkara, Surya P. Ayalasomayajula, Cheruku S. Rao, Jonathan L. Vennerstrom, Uday B. Kompella

Department of Pharmacal Sciences, Auburn University, Auburn, AL 36849, USA

Jack DeRuiter

Department of Ophthalmology, University of Nebraska Medical Center, Omaha, NE 68198-6025, USA

Uday B. Kompella

Correspondence: U. B. Kompella, Department of Pharmaceutical Sciences, University of Nebraska Medical Center, Omaha, NE 68198-6025, USA.
E-mail: ukompell@unmc.edu

Funding: This work was supported in part by the NIH grant EY11777 and UNMC graduate fellowships to Gangadhar Sunkara and Surya P. Ayalasomayajula.
For citation of meeting abstracts where the work was previously presented, see Gangadhar Sunkara (2002) *Transport, pharmacokinetics and ocular delivery of* N-*4-((benzoylamino) phenylsulfonyl)glycine, an aldose reductase inhibitor.* PhD Dissertation, Unversity of Nebraska Medical Center.

Introduction

Even with regular insulin treatment or oral hypoglycaemics in combination with an appropriate diet, exercise and the best clinical management (The Diabetes Control and Complications Trial Research Group 1993), current therapy in both insulin-dependent and non-insulin-dependent diabetic subjects is associated with significant morbidity and mortality due to diabetic complications (Ljubimov et al 1996a, b).

In hyperglycaemia, the glucose flux through the aldose reductase (AR) pathway is elevated, leading to polyol accumulation, glutathione depletion and myo-inositol depletion, which, in turn, results in diabetic complications. In diabetic patients, accumulation of sugar alcohol and AR activity in lens epithelial cells (Bron et al 1993), pericytes of retinal vessels (Akagi et al 1983) and corneal endothelial cells (Datiles et al 1983) has been correlated with the onset and progression of ocular diabetic complications, such as cataract, retinopathy and corneal epitheliopathy, respectively. Indeed, AR inhibitors have been shown to be useful in the treatment of ocular diabetic complications (Yabe-Nishimura 1998; Costantino et al 1999). In the past two decades, several groups developed a number of AR inhibitors (ARIs), but none of them is marketed in the USA due to the failure of some clinically tested ARIs. The reasons suggested for their failure include their poor safety, poor pharmacokinetics

and unrealistic clinical end points (Pfeifer et al 1997). Poor safety is associated with structure-related toxicity or non-specific inhibition of other members of the oxido-reductase family of enzymes. For example, the ARIs sorbinil, tolrestat and alrestatin were efficacious but caused severe side effects in a small patient population. Sorbinil caused hypersensitivity reactions similar to diphenylhydantoin (Pitts et al 1986; Sarges et al 1988) and it was speculated that the hydantoin moiety common to sorbinil and diphenylhydantoin was the cause for this hypersensitivity (Jaspan et al 1985). With tolrestat, the major side effect was hepatic damage with concomitant elevation of liver enzymes in 2% of the patients (Macleod et al 1992). With alrestatin, increased liver transaminases, severe liver reaction, leucopenia and photosensitive skin rashes were reported (Fagius & Jameson 1981; Handelsman & Turtle 1981). These side effects were attributed to non-specific inhibition of a similar oxido-reductase family of enzymes, such as aldehyde reductase and alcohol dehydrogenase, by these ARIs (Sato & Kador 1990; Pfeifer et al 1997; Oates & Mylari 1999). Thus, the above-listed compounds, or their analogues, were not preferred choices in the long-term treatment of diabetic complications. Hence, the primary challenge in the development of ARIs is to obtain a compound that selectively inhibits the AR enzyme and is devoid of toxic effects. Although ARIs showed considerable promise based on their intrinsic potency, their pharmacokinetics were apparently suboptimal, with drugs such as ponalrestat inadequately reaching the target tissues at clinically tested doses (Ziegler et al 1991; Krentz et al 1992). Thus, the other challenge in the development of ARIs is to obtain a compound with adequate availability in the target tissues.

In the quest for a potent, AR-specific, and well-permeable ARI, benzoyl amino phenyl sulfonyl glycines (BAPSGs) and benzoyl *N*-phenyl glycines (BNPGs) were developed (Mayfield & DeRuiter 1987). Among these two series of molecules, we selected *N*-4-[(benzoylaminophenyl)sulfonyl]glycine for further development based on its high in-vitro potency and permeability across ocular barriers such as the cornea and conjunctiva (Sunkara et al 2000). Furthermore, we demonstrated that BAPSG has ARI activity in cultured retinal pigment epithelial cells and in-vivo (Aukunuru et al 2002).

BAPSG is likely to be safe, due to the lack of a hydantoin moiety in its structure and due to its high selectivity for AR compared with other similar oxido-reductase families of enzymes (Davis et al 1993). BAPSG is a small molecular drug (MW = 334.35) that is anionic at physiological conditions ($pK_a = 3.35$; log P = 1.09). In addition, BAPSG interacts with anionic efflux transporters (Aukunuru et al 2001). To design approaches for delivering BAPSG to its target tissues, it is essential to understand the pharmacokinetics of BAPSG. Therefore, we investigated the plasma pharmacokinetics of BAPSG after intravenous, intraperitoneal and oral dosing and tissue distribution following intraperitoneal administration in Sprague-Dawley rats, and ocular tissue distribution after topical administration in rabbits.

Materials and Methods

Chemicals

The chemicals for BAPSG synthesis, including benzanilide, chlorosulfonic acid, carbon tetrachloride, ethyl acetate, sodium hydroxide and glycine, were bought from Sigma-Aldrich (St Louis, MO). Propylene glycol and dimethyl sulfoxide (DMSO) were purchased from Fisher Scientific (Philadelphia, PA). The β-hydroxy cyclodextrin was a gift from Cerestar USA Inc. (IN). Sodium sulfate, glacial acetic acid, HPLC-grade acetonitrile and methanol were purchased from Spectrum laboratories (CA).

BAPSG synthesis

BAPSG was prepared in two steps from benzanilide according to the method of Mayfield & DeRuiter (1987) with minor modifications. Chlorosulfonylation of benzanilide with chlorosulfonic acid gave 4-benzoylaminophenylsulfonyl chloride (BAPS-Cl), which upon treatment with glycine formed BAPSG. Each of these products was characterized using proton NMR, mass spectrometry and melting point analysis.

BAPSG formulation

BAPSG formulations were prepared just before dosing the animals. For intravenous pharmacokinetic studies, BAPSG solutions of appropriate concentration were made in saline containing 10% DMSO and 10% propylene glycol, and the injection volume did not exceed 100 μL for the dose ranges studied. For oral and intraperitoneal pharmacokinetic studies, an appropriate amount of BAPSG was placed in phosphate-buffered saline (pH 7.4) and sonicated for 5 min to obtain a suspension. The dosing volumes for these studies were in the range 500–1000 μL. For topical administration studies in rabbits, 5% w/v hydroxypropyl-β-cyclodextrin (50 mg mL^{-1}) was used to obtain a 5 mg mL^{-1} solution of BAPSG (15 mM).

Plasma and tissue disposition studies

Male Sprague-Dawley rats, 150–250 g, were purchased from SASCO (Wilmington, MA). The rats were maintained at the vivarium of University of Nebraska Medical Center as per the NIH guide for the care and use of laboratory animals. During the intravenous and intraperitoneal studies, rats were allowed free access to feed and water. However, for oral dosing studies, rats were fasted overnight and free access to feed and water was allowed after dosing.

Male New Zealand White rabbits, 2.5–3.5 kg, were obtained from Knapp Creek Rabbitory (Amana, IA). All rabbits were handled in accordance with the Guiding Principles in the Care and Use of Animals (DHEW publication, NK 80-23).

Plasma disposition studies in rats

BAPSG was injected intravenously via the tail vein and intraperitoneally at doses of 5, 15 and 50 mg kg^{-1}. In the oral pharmacokinetic study, BAPSG was administered by oral gavage at a dose of 15 mg kg^{-1}. In all these experiments, 200 μL of blood was collected at pre-determined time intervals and the plasma was separated. Plasma samples were stored at −20 °C until assayed for BAPSG. All plasma samples were analysed using an HPLC assay.

Plasma samples obtained from rat pharmacokinetic studies were processed and analysed for BAPSG. Each plasma sample (100 μL) was fortified with 1 μg of internal standard (10 μL of 100 μg mL^{-1} 4-fluoro-BAPSG) and extracted with 1 mL of extraction solvent (acetonitrile–methanol, 50:50 v/v). The mixture was vortexed for 15 min and centrifuged at 1500 *g* for 15 min. The supernatant containing BAPSG in the extraction solvent mixture was separated and evaporated under a stream of nitrogen gas (N-EVAP; Organomotion Associates, Berlin, MA). The resultant dried residue was reconstituted in 100 μL of mobile phase and the samples were injected onto a C-18 column (Microsrob; 25 × 4.5 cm, 100 Å, 5 μm). The mobile phase was a mixture of aqueous buffer (15 g of sodium sulfate dissolved in 1 L of 1% v/v acetic acid), acetonitrile and methanol (60:20:20 v/v), which was delivered at a flow rate of 1 mL min^{-1}. BAPSG and internal standards were monitored at 275 nm using a photodiode array detector, and their retention times were approximately 9.0 and 12.2 min, respectively. The lower limit of quantification (LOQ) of the assay was 25 ng mL^{-1} and the limit of detection (LOD) was 1 ng. Linear standard graphs of BAPSG were obtained in the concentration range of 25 ng mL^{-1} to 100 μg mL^{-1}, and the relative standard deviation between the assays was less than 7%. Concentrations below LOQ were reported as non-detectable and considered to be zero for the pharmacokinetic data analysis.

Tissue disposition study in rats

Following intraperitoneal administration of BAPSG (50 mg kg^{-1}), rats were sacrificed at 15 min or at 1, 2 and 4 h. Three rats were sacrificed at each time point and blood, brain, eye, liver, spleen, kidney, lungs and heart were isolated. Before harvesting the tissues, blood was collected and drained by cardiac puncture. From each eye, the cornea, lens and retina were isolated. Two eye tissues from each rat were pooled, weighed, homogenized in 100 μL of isotonic saline and the total volume of the homogenate was recorded. All other tissues were rinsed with saline and blotted to remove any adhering tissues or blood. Tissues were weighed and homogenized in approximately 2 volumes of isotonic saline and the final volumes of homogenates were recorded. Samples of homogenates were fortified with internal standard and extracted. The amount of BAPSG in each tissue was normalized to the wet weight of the tissue.

BAPSG was determined in the rat tissue homogenates. One hundred microliters of rat cornea, lens and retina homogenates were processed similar to plasma. For the analysis of BAPSG in rat kidney, heart, brain, liver and spleen, 500 μL of tissue homogenate was fortified with 1 μg of 4-F-BAPSG, and extracted with 2 mL of acetonitrile–methanol (50:50 v/v). The samples were vortexed for 15 min and centrifuged to separate the cell debris. The supernatants were collected and processed as described above for the rat plasma samples. Standard graphs were obtained in the concentration range of 25 ng mL^{-1} to 100 μg mL^{-1} after spiking known concentrations of BAPSG in blank tissue homogenates.

Plasma protein binding

Freshly obtained plasma from rats was fortified with BAPSG at 10, 50, 100 and 500 μg mL^{-1} and incubated for 1 h at 37 °C. Samples (300 μL) were transferred to pre-warmed Centrifree micropartition tubes (Amicon, Danvers, MA) and centrifuged at 1500 *g* in a temperature-controlled centrifuge (Beckman, Palo Alto, CA) for 30 min at 37 °C. The ultrafiltrates were treated similar to the rat plasma samples for BAPSG extraction and subsequent analysis using HPLC. The binding results were expressed as the fraction free or bound.

Ocular tissue disposition study in rabbits

Thirty microliters of BAPSG (5 mg mL^{-1}) dosing solution was instilled into the conjunctival cul-de-sac of each eye. At 30, 60, 120 and 180 min post-dosing, the rabbits were sacrificed with a marginal ear vein injection of 150 mg kg^{-1} sodium pentobaribital (Sleepaway, Fort Dodge, IA). The corneal and conjunctival surfaces were rinsed thoroughly with normal saline and blotted dry. The ocular tissues, including cornea, conjunctiva, iris-ciliary body, lens, aqueous humour and vitreous humour, were collected in pre-weighed microtubes, weighed and stored immediately at −70 °C. Aqueous humour (50 μL) was directly injected onto the HPLC column. All other tissues were minced and 2 mL of acetonitrile–methanol (50:50 v/v) was added to the finely ground tissue mass, which was then placed in a shaker for 6 h at 20 °C (cold extraction). The samples were then vortexed thoroughly for 5 min and centrifuged at 3000 g for 10 min. The supernatant (1.5 mL) was collected in test tubes and the organic layer was dried under N_2 gas. The dried supernatant was reconstituted with 100 μL of mobile phase and 50 μL was injected onto an HPLC column.

Pharmacokinetic data analysis

The plasma concentration–time profiles of BAPSG were analysed using Winnonlin (version 1.5, Scientific Consulting, Inc.) and the fit of the data to the selected model was statistically assessed using the minimum Akaike's information criterion estimation (Yamaoka et al 1978). The area under the plasma concentration–time curve ($AUC_{0\rightarrow last}$) was calculated by the linear trapezoidal rule and the area from the last concentration point (C_{last}) to infinity was calculated as C_{last}/K_e, where K_e was the rate constant obtained from the terminal phase. The apparent volume of distribution (V_d) and half-life ($t_{1/2}$) were determined from the intravenous data. The total body clearance (CL_T) was calculated as the dose divided by $AUC_{0\rightarrow\infty}$. Fraction

bioavailability (F) after oral and intraperitoneal administration was determined as the ratio of the $AUC_{0\rightarrow\infty}$ obtained from oral or intraperitoneal dosing to that obtained after intravenous administration of the same dose.

Statistical methods

Data are expressed as mean ± s.d, n = 3–6. The means between the groups were compared using analysis of variance and specific comparisons were made using Tukey's post-hoc analysis (SPSS, version 11.5). Differences were considered statistically significant at $P < 0.05$. Comparisons were made between different doses for each route (i.p. and i.v.) for plasma pharmacokinetics. Different incubation concentrations in the plasma protein binding study were compared for % free drug and % bound drug. Also, the drug AUCs in various tissues were compared following intraperitoneal administration in rats and topical administration in rabbits.

Results

Plasma disposition of BAPSG in rats

The plasma concentration-vs-time profiles of BAPSG following intravenous and intraperitoneal administration in rats are shown in Figures 1A and 1B, respectively. Table 1 summarizes the pharmacokinetic parameters obtained using non-compartmental analysis following intravenous and intraperitoneal administration. Plasma concentration-vs-time profiles of intravenous data were also subjected to compartmental analysis. Non-linear least square regression analyses of all data sets of intravenous data at three different dose levels indicated that BAPSG disposition can be described best by a one-compartment open model with first-order elimination at the 5 and 15 mg kg^{-1} doses, and a two-compartment open model with first-order elimination at the 50 mg kg^{-1} dose. Pharmacokinetic parameters obtained from non-compartmental analysis were used for the comparison of dose dependency and to estimate fraction bioavailability following different routes of administration. Due to erratic and poor absorption (Figure 2), pharmacokinetic parameters of BAPSG could not be obtained following oral administration. However, $AUC_{0\rightarrow\infty}$ was calculated using the linear trapezoid rule and terminal elimination half-life obtained from the intravenous data.

Following intraperitoneal and intravenous administration, no significant differences were observed in either C_{max} or $AUC_{0\rightarrow\infty}$, when these parameters were normalized to the dose administered (Table 1). Linear relationships were observed between both C_{max} and dose ($r^2 = 0.998$) and between $AUC_{0\rightarrow\infty}$ and dose ($r^2 = 0.998$) following intravenous administration. Similarly, linear relationships were observed between C_{max} and dose ($r^2 = 0.928$) and between $AUC_{0\rightarrow\infty}$ and dose ($r^2 = 0.976$) following intraperitoneal administration. The linear correlation between dose and $AUC_{0\rightarrow\infty}$ following intravenous and intraperitoneal administration is shown in Figure 1C. To evaluate the bioavailability (F) following intraperitoneal administration, the mean $AUC_{0\rightarrow\infty}$ of the individual intraperitoneal data sets within a dosage group were compared with intravenous data sets for the corresponding dose group. F estimates following intraperitoneal administration ranged from 0.7 to 1 for the three doses. Orally administered BAPSG (15 mg kg^{-1}) exhibited an erratic pharmacokinetic profile and poor bioavailability (6.1 ± 3.2%) (Figure 2).

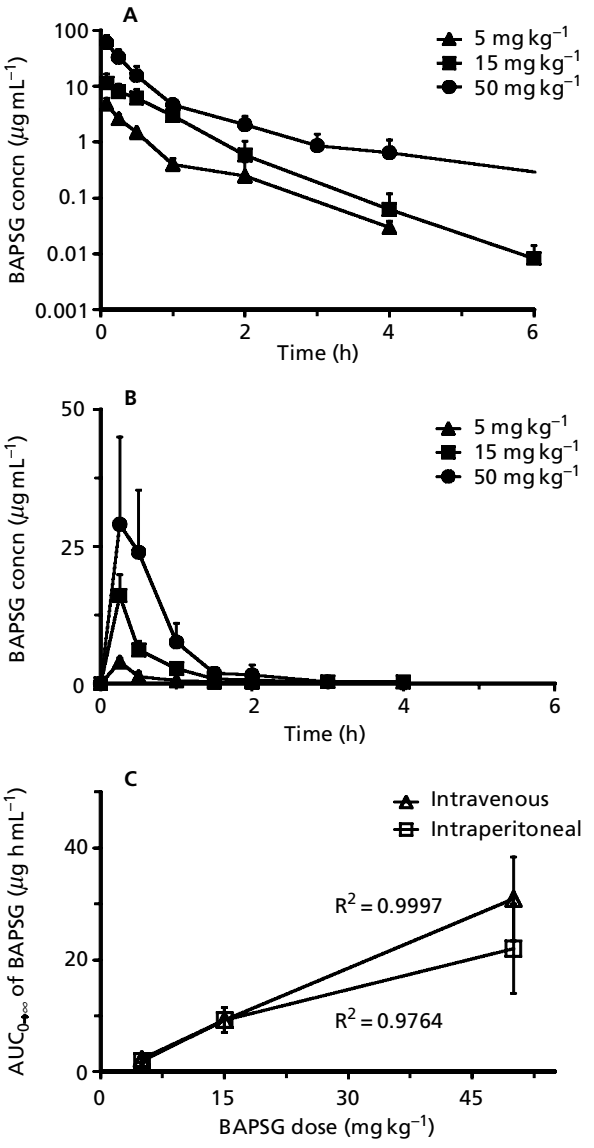

Figure 1 The plasma concentration-vs-time profiles of BAPSG following intravenous (A) and intraperitoneal (B) administration and plasma $AUC_{0\rightarrow\infty}$ dose relationship (C) following intravenous and intraperitoneal administrations of BAPSG in rats. The data are expressed as mean ± s.d. for n = 3–6 rats.

Tissue disposition of BAPSG in rats

In the tissue distribution study, BAPSG levels were estimated in cornea, lens, retina, brain, kidney, heart, liver and spleen at 15 min and 1, 2 and 4 h post dosing (50 mg kg^{-1}, i.p.).

Table 1 Pharmacokinetic parameters of BAPSG in rats following intravenous and intraperitoneal administration at three different doses.

Parameter	Intravenous			Intraperitoneal		
	5 mg kg^{-1}	15 mg kg^{-1}	50 mg kg^{-1}	5 mg kg^{-1}	15 mg kg^{-1}	50 mg kg^{-1}
C_0 (μg mL^{-1})	6.24 ± 1.83	14.54 ± 9.01	81.17 ± 35.10*†	—	—	—
C_{max} (μg mL^{-1})	—	—	—	3.94 ± 0.70	16.01 ± 4.78*	39.84 ± 15.4*†
T_{max} (h)	—	—	—	0.25 ± 0.00	0.33 ± 0.14	0.30 ± 0.11
$t_{½}$(h)	0.54 ± 0.14	0.68 ± 0.3	1.49 ± 0.83	0.41 ± 0.05	0.70 ± 0.04*	1.99 ± 1.30
$AUC_{0-\infty}$ (μg h mL^{-1})	2.76 ± 0.63	9.22 ± 2.24*	30.95 ± 7.50*†	2.01 ± 0.46	9.38 ± 2.46*	23.3 ± 11.3*†
AUC_{0-last} (μg h mL^{-1})	2.8 ± 0.6	9.21 ± 2.24*	30.83 ± 7.40*†	1.86 ± 0.41	9.05 ± 2.40*	21.88 ± 8.04*†
F	1.00 ± 0.26	1.00 ± 0.24	1.00 ± 0.24	0.88 ± 0.20	1.00 ± 0.24	0.7 ± 0.3
V_d/F (L)	0.25 ± 0.06	0.27 ± 0.18	2.15 ± 0.70*†	0.37 ± 0.04	0.43 ± 0.14	0.61 ± 0.21
CL_T/F (L h^{-1})	0.32 ± 0.07	0.26 ± 0.07	0.30 ± 0.08	0.65 ± 0.16	0.42 ± 0.11	3.32 ± 2.10*†
MRT (h)	0.59 ± 0.22	0.65 ± 0.23	1.30 ± 0.5*†	0.63 ± 0.14	0.86 ± 0.10	1.24 ± 0.37*†
C_0/dose	7.17 ± 2.10	5.28 ± 3.2	9.27 ± 4.01	—	—	—
C_{max}/dose (μg)	—	—	—	4.53 ± 0.80	5.8 ± 1.7	3.40 ± 1.76
$AUC_{0-\infty}$/dose	2.62 ± 0.68	2.62 ± 0.68	3.53 ± 0.88	2.37 ± 0.50	3.41 ± 0.88	2.7 ± 0.9

The data are presented as mean ± s.d. for n = 3–5 for intravenous route and 4–6 for intraperitoneal route. C_0 = concn at zero time; $t_{½}$ = half-life from the terminal phase; AUC = area under the curve; MRT = mean residence time ($AUMC_{0-\infty}/AUC_{0-\infty}$); V_d = apparent volume of distribution; F = fraction bioavailability; CL_T = total body clearance; T_{max} = time to reach maximum concn (C_{max}); *$P < 0.05$, 15 mg kg^{-1} vs 5 mg kg^{-1} or 50 mg kg^{-1} vs 5 mg kg^{-1}; †$P < 0.05$, 50 mg kg^{-1} vs 15 mg kg^{-1}.

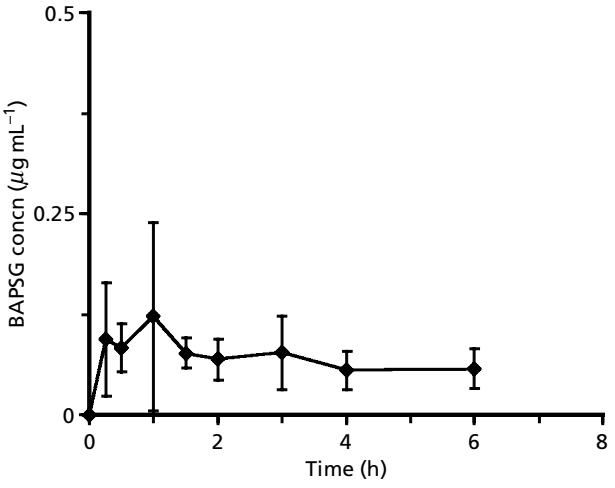

Figure 2 Plasma concentration of BAPSG following oral administration (15 mg kg^{-1}) in rats. The data are expressed as mean ± s.d. for n = 6 rats.

Table 2 Tissue exposure of BAPSG in rats following intraperitoneal administration at a dose of 50 mg kg^{-1}.

Tissue	AUC_{0-4h} (μg h g^{-1})[a]*	Tissue/plasma ratio[b]
Brain	0.05 ± 0.04[c]	0.002 ± 0.002
Retina	1.3 ± 0.7	0.06 ± 0.03
Cornea	4.2 ± 1.9	0.19 ± 0.09
Lens	0.30 ± 0.35	0.01 ± 0.02
Liver	10.97 ± 2.3	0.5 ± 0.1
Heart	1.73 ± 1.08	0.08 ± 0.05
Kidney	33.45 ± 6.60	1.54 ± 0.30
Spleen	1.83 ± 0.53	0.08 ± 0.02
Plasma	21.7 ± 4.0	1.00 ± 0.18

[a,b]The data are expressed as mean ± s.d. for n = 3 rats; [b]The ratio of the AUC_{0-4h} of the tissue to the mean AUC_{0-4h} of plasma; [c]BAPSG was not detectable in brain after 15 min. Brain AUC was determined by assuming other concentrations after 15 min as zero. *The statistically significant rank order of AUCs and the tissue/plasma AUC ratios was: kidney > plasma > liver > cornea ~ spleen ~ retina ~ heart ~ lens > brain.

BAPSG was detectable in the target ocular tissues – retina, lens and cornea. Tissue exposure of BAPSG expressed as AUC_{0-4h} (μg h g^{-1}) based on drug amounts (μg) per gram tissue, was in the order: kidney > plasma > liver > cornea ~ spleen ~ retina ~ heart ~ lens > brain (Table 2). Maximal levels of BAPSG were observed at 1 h after dosing in most of the tissues, and declined with time in all the tissues.

Plasma protein binding of BAPSG

Protein binding studies revealed that BAPSG was bound to rat plasma proteins and the free fraction in plasma was 0.12–16.7% (% bound, 83.2–99.8%) over a concentration range 10–500 μg mL^{-1} (Table 3). Although BAPSG is bound to rat plasma proteins, it has a volume distribution of greater than 1 L kg^{-1}, indicating high tissue affinity. For example, the ratio of kidney-to-plasma AUC_{0-4h} is more than 1, suggesting the affinity of BAPSG to the renal tissue (Table 2).

Ocular tissue disposition of BAPSG in rabbits

Following topical administration, ocular tissue disposition of a single dose of BAPSG was investigated in

Table 3 Rat plasma protein binding of BAPSG – free and bound fractions following BAPSG incubations at four different concentrations.

BAPSG concn ($\mu g\,mL^{-1}$)	% Free	% Bound
10	$0.12 \pm 0.22^{a\dagger}$	$99.80 \pm 0.22^{\dagger}$
50	$11.9 \pm 2.3^{*}$	$88.04 \pm 2.70^{*}$
100	$14.7 \pm 0.5^{*\dagger}$	$85.0 \pm 0.5^{*}$
500	$16.7 \pm 0.8^{*\dagger}$	$83.2 \pm 0.8^{*}$

The data are expressed as mean ± s.d. for n = 3. [a]BAPSG was below quantification limit in two of the three samples. $^{*}P < 0.05$ when compared with $10\,\mu g\,mL^{-1}$; $^{\dagger}P < 0.05$ when compared with $50\,\mu g\,mL^{-1}$.

rabbits. A 30-μL drop containing 150 μg of BAPSG was instilled into each eye and the drug levels were monitored at 30 min and 1, 2 and 3 h in cornea, conjunctiva, iris-ciliary body, aqueous humour, lens and vitreous humour. The kinetic profiles of BAPSG concentrations in various ocular tissues are shown in Figure 3, and the time to reach peak concentrations (T_{max}) and AUC_{0-3h} are shown in Table 4. Higher levels of BAPSG were observed in the ocular tissues that were in immediate contact with the dosing solution, namely the cornea and conjunctiva. At 30 min, the concentration of BAPSG ($\mu g\,g^{-1}$) was 1.74 ± 0.7, 0.7 ± 0.2, 0.10 ± 0.3, 0.09 ± 0.036 and 0.019 ± 0.002 in the cornea, conjunctiva, lens, iris-ciliary body and aqueous humour, respectively. After 30 min of administration, no BAPSG was detected in the lens. BAPSG was not detectable in vitreous humour up to 3 h. Tissue exposure (AUC_{0-3h}) was in the order: cornea > conjunctiva > iris-ciliary body > aqueous humour > lens (Table 4). Even after 3 h of administration, the BAPSG levels were high and sustained in the cornea (Figure 3A), suggesting that the residence time of the BAPSG was higher in the cornea possibly due to its affinity to the tissue. At all the sampling time points (0.5, 1, 2 and 3 h), blood levels of BAPSG were below detection limits. Tissue clearance parameters were not determined, as it was difficult to discern the terminal linear elimination phase in the tissues (Figure 3A).

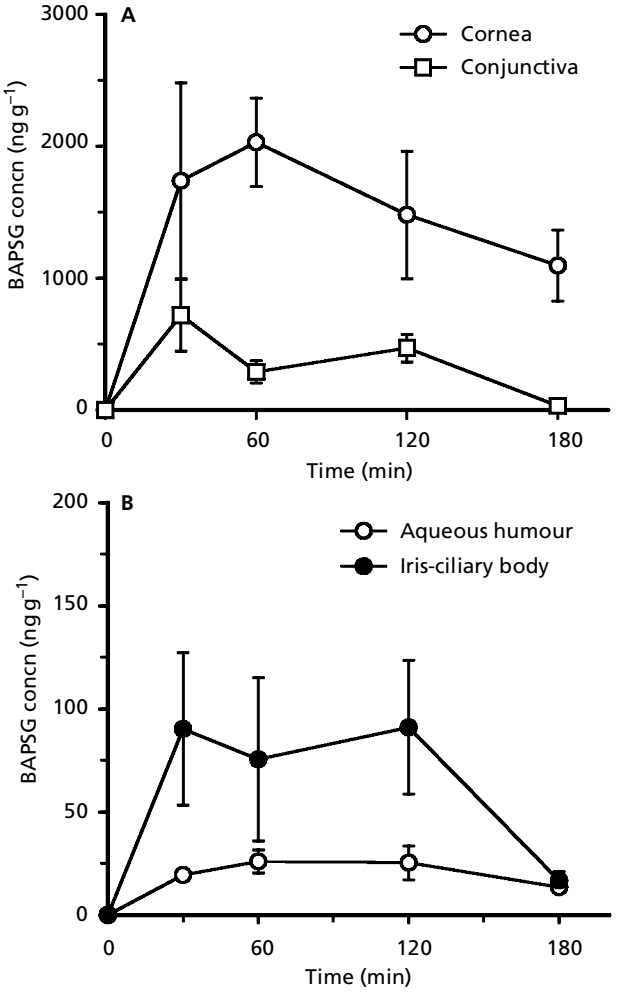

Figure 3 Ocular tissue concentration-vs-time profiles of BAPSG following topical administration (150 μg/eye) in rabbits. A. Profiles in the extra-ocular tissues – cornea and conjunctiva. B. Profiles in the intra-ocular tissues – aqueous humour and iris-ciliary body. The data are expressed as mean ± s.d. for n = 4 eyes.

Table 4 Ocular tissue exposure of BAPSG in rabbits following topical administration at a dose of 150 μg/eye.

Tissue	AUC_{0-3h} ($\mu g\,min\,g^{-1}$)[a]*	T_{max}[b] (min)
Cornea	290.81 ± 54.30	52.5 ± 15
Conjunctiva	63.75 ± 6.60	52.5 ± 45.0
Aqueous humour	3.70 ± 0.64	105 ± 30
Lens	ND[c]	ND[c]
Iris-ciliary body	34.31 ± 13.40	ND[d]

[a,b]The data are expressed as mean ± s.d. for n = 4 eyes; [b]T_{max} = the sampling time at which peak concentrations were observed; [c]BAPSG was not detectable in the lens after 30 min; [d]T_{max} could not be determined due to erratic profile; BAPSG was below quantification limit in the vitreous humour; retina was not collected; $^{*}P < 0.05$ (cornea > conjunctiva > iris-ciliary body > aqueous humour > lens).

Discussion

This study assessed the tissue disposition of BAPSG in rats and rabbits. Rats were used to investigate the disposition of BAPSG following intravenous, intraperitoneal and oral administration because rat models are widely used to understand the progression of diabetic complications of the eye (Alder et al 1998). Furthermore, the AR from rat lenses exhibits apparent K_m values similar to that in human lenses at both high and low concentrations of sugar substrates (Conrad & Doughty 1982). For drug disposition from eye drops, the rabbit is by far the most

commonly used animal model (Urtti & Salminen 1993). Therefore, the ocular tissue disposition of BAPSG was evaluated following single eye drop administration in rabbits.

The intravenous pharmacokinetic data indicated that BAPSG exhibits dose-proportionate AUCs with an elimination half-life of 0.5–1.5 h. The extrapolated plasma concentrations of BAPSG at 0 h (C_0) and the $AUC_{0\rightarrow\infty}$ normalized to dose were not different. In addition, the plasma clearance of BAPSG was not affected by dose. The bioavailability of BAPSG following intraperitoneal administration in rats was 70–100%. Absorption of BAPSG following intraperitoneal administration was rapid, and the plasma levels peaked at around 15 min. BAPSG exhibited dose-proportionate AUCs at 5, 15 and 50 mg kg^{-1} following intraperitoneal administration with a mean terminal elimination half-life of around 0.4–2 h. The oral absorption of BAPSG was found to be poor and erratic. The limited and erratic oral absorption of BAPSG may be due to its acidic nature ($pK_a = 3.35$), which may have caused its precipitation in the acidic pH conditions of the gastrointestinal tract.

Since the systemic bioavailability of BAPSG after intraperitoneal administration is almost complete, this route was used for the tissue disposition studies. It is noteworthy that systemic administration could deliver the anionic BAPSG to all the target tissues in the eye – retina, lens and cornea. Especially interesting is the observation that the cornea/plasma distribution ratio is comparable or higher than that in the heart and spleen. The tissue-to-plasma AUC_{0-4h} ratio of BAPSG was 0.06 in the retina and much less in the brain (Table 2), suggesting the greater ability of BAPSG to cross the blood–retinal barrier compared with the blood–brain barrier. Alternatively, the efflux of BAPSG by anionic drug efflux pumps, such as multidrug-resistance-associated protein (MRP), which are present in the brain microvessel endothelial cells (Zhang et al 2000; Aukunuru et al 2001), may account for the very low accumulation of BAPSG in the retina. Since MRP is also known to be present in the retinal pigment epithelial cells and because BAPSG accumulation in these cells can be enhanced by MRP inhibitors (Aukunuru et al 2001), it will be interesting to determine whether retinal delivery of BAPSG can be enhanced by co-administration of MRP inhibitors. The blood–aqueous barrier is more permeable than the blood–retinal barrier, and once the drug enters the aqueous humour after crossing the blood–aqueous barrier it is readily available to the lens (Sunkara & Kompella 2003). Also, the drug present in the vitreous can access the lens. However, the lens/plasma distribution of BAPSG was 0.01. This low ratio is possibly because the drug from aqueous may be removed by the cornea, which appears to have greater affinity for the drug. Another interesting property of BAPSG revealed in these studies is its preferential distribution to the kidneys, a target for drugs, such as ARIs, that are capable of preventing diabetic nephropathy.

Since BAPSG is of potential value in treating ocular diabetic complications, such as corneal epitheliopathy, cataract and retinopathy, and because topical administration is a convenient approach, the ocular tissue disposition following single dose topical administration (as eye drop) of BAPSG was investigated in rabbits. We observed no BAPSG in the lens at 30 min post-dosing. The overall lens exposure of BAPSG was significantly lower than for the cornea, conjunctiva and aqueous humour and BAPSG was not detectable in vitreous humour up to 3 h. The drug exposures to iris-ciliary body and aqueous humour were less compared with the cornea and conjunctiva, possibly due to the limiting nature of the corneal and conjunctival barriers. BAPSG levels in the cornea were high and prolonged for 3 h, suggesting that the residence time of BAPSG is higher in the cornea probably due to its affinity to this tissue. The systemic exposure of BAPSG following topical administration was negligible. These results suggest that BAPSG concentrations in the extra-ocular tissues, after topical administration, are relatively higher than the levels in intra-ocular tissues. BAPSG exists as charged species at physiological pH conditions (>99% exists as the ionized form). The presence of a carboxylic acid group (-COOH) in the chemical structure of BAPSG is responsible for its low pK_a and high degree of ionization. Reducing the degree of ionization of BAPSG by chemical derivatization, such as esterification, may enhance its lipophilicity and the transport across lipophilic cornea, thereby enhancing its delivery to the lens. However, our earlier studies indicated a reduction in the in-vitro transport and in-vivo uptake of the drug, upon ester prodrug formation (Sunkara et al 2000). This was attributed to the possible existence of carrier-mediated transport for the corneal entry of BAPSG.

In both rat and rabbit, BAPSG appears to have low affinity for the lens and high affinity for the cornea. Systemic mode of administration delivered significant drug levels to all target tissues in the eye for diabetic complications. However, the topical route appears much less efficient in delivering BAPSG to the intra-ocular tissues or the systemic circulation. Thus, systemic mode of administration is a feasible approach to deliver BAPSG to the various ocular tissues, as well other tissues such as kidneys, that are affected by diabetic complications. This is consistent with the AR inhibitory activity, oxidative stress and VEGF inhibitory effect, and anti-cataract effect that we previously observed for BAPSG following subcutaneous mode of administration in a rat model (Aukunuru et al 2002).

In summary, plasma pharmacokinetics of BAPSG in rats can be described with a one-compartment open model with first-order elimination at doses 5 and 15 mg kg^{-1} and 2-compartment open model with first-order elimination at 50 mg kg^{-1}. BAPSG has an elimination half-life of 0.5–1.5 h. BAPSG is poorly available following oral administration (~6%) and its bioavailability is nearly complete following intraperitoneal administration in rats. Even though BAPSG is highly bound to plasma proteins, its high volume of distribution (>1 L kg^{-1}) suggests its affinity to the tissues. Tissue disposition studies indicated that BAPSG reaches the retina, lens and cornea following systemic administration in rats. After topical administration in rabbits, BAPSG was not detectable after 30 min in the lens and

did not reach the vitreous, while significant drug levels were seen in the cornea and conjunctiva even at 3 h.

References

Akagi, Y., Kador, P. F., Kuwabara, T., Kinoshita, J. H. (1983) Aldose reductase localization in human retinal mural cells. *Invest. Ophthalmol. Vis. Sci.* **24**: 1516–1519

Alder, V. A., Su, E. N., Yu, D. Y., Cringle, S., Yu, P. (1998) Overview of studies on metabolic and vascular regulatory changes in early diabetic retinopathy. *Aust. N. Z. J. Ophthalmol.* **26**: 141–148

Aukunuru, J. V., Sunkara, G., Bandi, N., Thoreson, W. B., Kompella, U. B. (2001) Expression of multidrug resistance-associated protein (MRP) in human retinal pigment epithelial cells and its interaction with BAPSG, a novel aldose reductase inhibitor. *Pharm. Res.* **18**: 565–572

Aukunuru, J. V., Sunkara, G., Ayalasomayajula, S. P., DeRuiter, J., Clark, R. C., Kompella, U. B. (2002) A biodegradable injectable implant sustains systemic and ocular delivery of an aldose reductase inhibitor and ameliorates biochemical changes in a galactose-fed rat model for diabetic complications. *Pharm. Res.* **19**: 278–285

Bron, A. J., Sparrow, J., Brown, N. A., Harding, J. J., Blakytny, R. (1993) The lens in diabetes. *Eye* **7** (Pt 2): 260–275

Conrad, S. M., Doughty, C. C. (1982) Comparative studies on aldose reductase from bovine, rat and human lens. *Biochim. Biophys. Acta* **708**: 348–357

Costantino, L., Rastelli, G., Vianello, P., Cignarella, G., Barlocco, D. (1999) Diabetes complications and their potential prevention: aldose reductase inhibition and other approaches. *Med. Res. Rev.* **19**: 3–23

Datiles, M. B., Kador, P. F., Fukui, H. N., Hu, T. S., Kinoshita, J. H. (1983) Corneal re-epithelialization in galactosemic rats. *Invest. Ophthalmol. Vis. Sci.* **24**: 563–569

Davis, R. A., Mayfield, C. A., Aull, J. L., DeRuiter, J. (1993) Enzyme selectivity analyses of arylsulfonylamino acid aldose reductase inhibitors. *J. Enzyme Inhib.* **7**: 87–96

Fagius, J., Jameson, S. (1981) Effects of aldose reductase inhibitor treatment in diabetic polyneuropathy – a clinical and neurophysiological study. *J. Neurol. Neurosurg. Psychiatry* **44**: 991–1001

Handelsman, D. J., Turtle, J. R. (1981) Clinical trial of an aldose reductase inhibitor in diabetic neuropathy. *Diabetes* **30**: 459–464

Jaspan, J. B., Herold, K., Bartkus, C. (1985) Effects of sorbinil therapy in diabetic patients with painful peripheral neuropathy and autonomic neuropathy. *Am. J. Med.* **79**: 24–37

Krentz, A. J., Honigsberger, L., Ellis, S. H., Hardman, M., Nattrass, M. (1992) A 12-month randomized controlled study of the aldose reductase inhibitor ponalrestat in patients with chronic symptomatic diabetic neuropathy. *Diabet. Med.* **9**: 463–468

Ljubimov, A. V., Burgeson, R. E., Butkowski, R. J., Couchman, J. R., Wu, R. R., Ninomiya, Y., Sado, Y., Maguen, E., Nesburn, A. B., Kenney, M. C. (1996a) Extracellular matrix alterations in human corneas with bullous keratopathy. *Invest. Ophthalmol. Vis. Sci.* **37**: 997–1007

Ljubimov, A. V., Burgeson, R. E., Butkowski, R. J., Couchman, J. R., Zardi, L., Ninomiya, Y., Sado, Y., Huang, Z. S., Nesburn, A. B., Kenney, M. C. (1996b) Basement membrane abnormalities in human eyes with diabetic retinopathy. *J. Histochem. Cytochem.* **44**: 1469–1479

Macleod, A. F., Boulton, A. J., Owens, D. R., Van Rooy, P., Van Gerven, J. M., Macrury, S., Scarpello, J. H., Segers, O., Heller, S. R., Van Der Veen, E. A. (1992) A multicentre trial of the aldose-reductase inhibitor tolrestat, in patients with symptomatic diabetic peripheral neuropathy. North European Tolrestat Study Group. *Diabetes Metab.* **18**: 14–20

Mayfield, C. A., DeRuiter, J. (1987) Novel inhibitors of rat lens aldose reductase: N-[[(substituted amino)phenyl]sulfonyl] glycines. *J. Med. Chem.* **30**: 1595–1598

Oates, P. J., Mylari, B. L. (1999) Aldose reductase inhibitors: therapeutic implications for diabetic complications. *Expert Opin. Investig. Drugs* **8**: 2095–2119

Pfeifer, M. A., Schumer, M. P., Gelber, D. A. (1997) Aldose reductase inhibitors: the end of an era or the need for different trial designs? *Diabetes* **46** (Suppl. 2): S82–S89

Pitts, N. E., Vreeland, F., Shaw, G. L., Peterson, M. J., Mehta, D. J., Collier, J., Gundersen, K. (1986) Clinical experience with sorbinil – an aldose reductase inhibitor. *Metabolism* **35**: 96–100

Sarges, R., Schnur, R. C., Belletire, J. L., Peterson, M. J. (1988) Spiro hydantoin aldose reductase inhibitors. *J. Med. Chem.* **31**: 230–243

Sato, S., Kador, P. F. (1990) Inhibition of aldehyde reductase by aldose reductase inhibitors. *Biochem. Pharmacol.* **40**: 1033–1042

Sunkara, G., Kompella, U. B. (2003) Transport processes in ocular epithelia. In: Mitra, A. K. (ed.) *Ophthalmic drug delivery*. Marcel Dekker, New York, pp 13–58

Sunkara, G., Deruiter, J., Clark, C. R., Kompella, U. B. (2000) In-vitro hydrolysis, permeability, and ocular uptake of prodrugs of N-[4-(benzoylamino)phenylsulfonyl]glycine, a novel aldose reductase inhibitor. *J. Pharm. Pharmacol.* **52**: 1113–1122

The Diabetes Control and Complications Trial Research Group (1993) The effect of intensive treatment of diabetes on the development and progression of long-term complications in insulin-dependent diabetes mellitus. *N. Engl. J. Med.* **329**: 977–986

Urtti, A., Salminen, L. (1993) Animal pharmacokinetic studies. In: Mitra, A. K. (ed.) *Ophthalmic drug delivery systems*. Marcel Dekker, New York, pp 317–375

Yabe-Nishimura, C. (1998) Aldose reductase in glucose toxicity: a potential target for the prevention of diabetic complications. *Pharmacol. Rev.* **50**: 21–33

Yamaoka, K., Nakagawa, T., Uno, T. (1978) Statistical moments in pharmacokinetics. *J. Pharmacokinet. Biopharm.* **6**: 547–558

Zhang, Y., Han, H., Elmquist, W. F., Miller, D. W. (2000) Expression of various multidrug resistance-associated protein (MRP) homologues in brain microvessel endothelial cells. *Brain Res.* **876**: 148–153

Ziegler, D., Mayer, P., Rathmann, W., Gries, F. A. (1991) One-year treatment with the aldose reductase inhibitor, ponalrestat, in diabetic neuropathy. *Diabetes Res. Clin. Pract.* **14**: 63–73